

**Ruthenium Volatilisation in Nuclear Waste Systems –Comparison of
Ru^(III)Cl₃ and Ru^(III)NO(NO₃)₃
17113**

Sukhraaj K. Johal¹, Colin Boxall^{1*}, Colin Gregson², Carl J. Steele³

¹The Lloyd's Register Foundation Centre for Nuclear Engineering, Engineering Department, Lancaster University, Bailrigg, Lancashire, LA1 4YR, U.K.

²National Nuclear Laboratory, Sellafield, Seascale, Cumbria, CA20 1PG, U.K.

³Sellafield Ltd., Sellafield, Seascale, Cumbria, CA20 1PG, U.K.

ABSTRACT

Ruthenium is a fission product possessed of two relatively long lived isotopes; ¹⁰³Ru and ¹⁰⁶Ru, both of which form part of the Highly Active (HA) waste raffinate during spent nuclear fuel reprocessing. During reprocessing, ruthenium, which may be in the form of the RuNO³⁺ complex, encounters temperatures conducive to volatilisation. Due to ruthenium's high specific radioactivity it is important to understand the mechanism by which volatilisation occurs. Here we use combined cyclic voltammetry (CV) and electrochemical microgravimetry experiments in a study of both NO free Ru (III), in the form of a RuCl₃ solution and NO complexed Ru (III), in the form of RuNO³⁺ solutions. We do this in order to establish baseline behaviour of NO free Ru (III) and compare it to NO complexed Ru (III) to determine the effect of complexation on the system. We have observed discrete oxidations in both systems from solution phase Ru (III) to solid phase RuO₂ and volatile RuO₄. Two key differences emerged between the two systems, the first being the mass changes associated with deposition and stripping of RuO₂ are significantly smaller in the RuNO³⁺ solutions than those for solutions of RuCl₃. The second difference is the difference in onset of volatile RuO₄ generation, in the RuNO³⁺ solution, RuO₄ generation is 100 mV positive than that for the RuCl₃ solution. This suggests NO complexation protects Ru (III) against oxidation and, to a certain extent, volatilisation as RuO₄.

INTRODUCTION

Spent nuclear fuel management at the UK's Sellafield reprocessing plants includes the reprocessing of spent nuclear fuel by the solvent extraction-based PUREX (Plutonium Uranium Redox EXtraction) process. This produces a Highly Active (HA) aqueous waste raffinate which is concentrated into evaporators and storage tanks in the Highly Active Liquor Evaporation and Storage (HALES) facility. From there, it is fed to the Waste Vitrification Plant (WVP) where the resultant Highly Active Liquor (HAL) feed is calcined and combined with glass to produce an immobilised HA waste form. Ruthenium is a fission product with 2 relatively long lived isotopes; ¹⁰³Ru and ¹⁰⁶Ru, $t_{1/2} = 39.8$ days and 1 year respectively, both isotopes form part of the wider inventory of fission products within the HA raffinate. Volatilisation of fission products in nuclear waste generally occurs at high temperature – apart from ruthenium where volatilisation occurs at the lower temperature stages of the three stage vitrification process. These are:

1. The HAL is evaporated to dryness
2. The solid residues are calcined (denitration to the oxides occurs in this stage)
3. The calcined oxides are fused into a glass melt.

Volatile Ru generation mainly occurs as the last of the liquid is removed and the material becomes a solid. Dust and other volatiles are removed from the vessel ventilation system via a dust scrubber, condenser and NO_x absorber (primary off-gas system) followed by an electrostatic precipitator (ESP), wet scrubber and two banks of HEPA filters (secondary off-gas system) to avoid release of radioactive isotopes (including ¹⁰⁶Ru and ¹⁰³Ru) to the environment via the WVP stack. However, given its volatile nature and high specific radioactivity ruthenium presents a strong challenge to the nuclear industry in effectively managing its abatement. Especially, vitrification at Sellafield has been scrutinised since the discharge of 3.1 GBq of volatile ¹⁰⁶Ru via the WVP in 1997. Thus, understanding the highly complex solution chemistry of ruthenium is essential as it is widely believed a redox state change from Ru (III) to Ru (VIII) is responsible for volatilisation of ruthenium via RuO₄ formation. (1-8)

Nitrite and nitrous acid are produced within the HAL by radiolysis of the concentrated nitric acid used in the PUREX aqueous process streams and thus the HA raffinate. However, neither is stable in acid solution, decomposing to form NO and NO₂ via N₂O₃. NO, in particular, forms a strong affiliation with Ru (III) (9) resulting in the formation of the nitrosyl ruthenium, Ru(NO)³⁺, species that is ubiquitous in HAL chemistry. The chemical mechanism of ruthenium changing from a solution species either as free Ru³⁺ or Ru(NO)³⁺, to a volatile form is poorly understood. Current assumptions (10) are that, in nitric acid media, ruthenium nitrosyl nitrates [Ru(NO)(NO₃)_x(H₂O)_{5-x}] where x = 3,4 are the most likely candidates to oxidise to volatile ruthenium, considered to be RuO₄ (vide supra). It is reported that in excess of 70% of ruthenium in solution can exist as [Ru(NO)(NO₃)₃₋₄(H₂O)₁₋₂] at high acidity. Furthermore, recent experimental work within the UK National Nuclear Laboratory (5) has demonstrated that the presence of oxidising metal ions in HA waste (e.g. Ce(IV)) can enhance the volatility of ruthenium through a chemical conversion of Ru(III) species to what is, again, assumed to be RuO₄.

A better understanding of these species, their electrochemical processes and reaction kinetics is required to underpin the empirical evidence gathered to date. Several studies have investigated the redox state changes of ruthenium in acid media, both in the presence and absence of nitrate. These are summarized in Table 1 and described as follows. Wehner and Hindman (11) investigated electrolytic preparation methods of Ru (III) and Ru (IV) and subsequent absorption spectra. They studied the electrochemical transition of the Ru (III) to Ru (IV) redox couple from a solution of Ru (IV) in various concentrations of HClO₄ prepared from the electrolytic reduction of RuO₄ solutions. They reported the formal potential of Ru (III) to Ru (IV) to lie in a range between 0.55 and 1.17 V vs. the normal hydrogen electrode (NHE). Consistent with this range, polarographic studies of the Ru (III) to Ru (IV) transition by Niedrach and Tevebaugh (12) quoted a value of 0.65 V vs. NHE for the standard electrode potential of Ru (III) to Ru (IV) in HClO₄. This value

was also in agreement with that obtained by Atwood and DeVries (13) from a polarography study of the reduction of Ru (IV) in HClO_4 , in which they obtained a value of 0.59 V vs. NHE.

Table I: Summary of formal potentials reported in the literature for key Ru redox transitions between Ru (III) and Ru (VIII) oxidation states. All potentials reported have been rescaled with reference to the SCE

Potential / V vs SCE	Assigned Process	Expt Details	Authors	Ref No
0.31-0.93	Ru(III)/Ru(IV) n=1	Oxidation on Au in HClO_4 at pH 0	Wehner & Hindman	(11)
0.41	Ru(III)/Ru(IV) n=1	Oxidation on Au in HClO_4 at pH 0	Niedrach & Tevebaugh	(12)
0.35	Ru(III)/Ru(IV) n=1	Reduction on Pt in HClO_4 at pH 1	Atwood & DeVries	(13)
0.15	Ru(3.5)/Ru(IV) n=0.5	Reduction on Pt in 0.9M NaNO_3 and 0.1M HNO_3	Maya	(14)
0.35	Ru(3.75)/Ru(IV) n=0.25	Reduction on Pt in 0.9M NaNO_3 and 0.1M HNO_3	Maya	(14)
0.92	Ru(IV)/Ru(4.38) n=0.38	Reduction on Pt in 0.9M NaNO_3 and 0.1M HNO_3	Maya	(14)
0.96	Formation of Ru(4.38) from Ru(VI)	Oxidation on Pt in HClO_4 at pH 0	Wehner & Hindman	(11)
1.16	Formation of Ru(VIII) from Ru(IV)	Irreversible oxidation on Pt in HClO_4 at pH 0	Wehner & Hindman	(11)
0.395	Ru(IV)/Ru(3.75)	Reduction on Au in HNO_3 at pH -0.5	Mousset	(10)
0.895	Ru(IV)/Ru(4.38)	Reduction on Au in HNO_3 at pH -0.5	Mousset	(10)
1.095	Ru(III)/Ru(VIII)	Oxidation on Au in HNO_3 at pH 3	Mousset	(10)
1.495	Ru(III)/Ru(VIII)	Oxidation on Au in HNO_3 at pH 3	Mousset	(10)

More recently, Maya (14) studied the reduction of Ru (IV), prepared from the photolytic dissociation of ruthenium nitrosyl nitrate solutions to Ru (III) solutions, these were allowed to spontaneously oxidise up to Ru (IV). These were in the form of $\text{Ru}_4(\text{OH})_{12}^{4+}$ in a $\text{HNO}_3/\text{NaNO}_3$ mixture and Maya reported reduction peaks at 0.15, 0.35, 0.92 V vs. saturated calomel electrode (SCE) which they attribute to tetramer chemistry. These features were also observed by Wallace and Propst (15) and were within 10 mV of the values reported by Maya. It was found each process involved a 1 e⁻ transfer corresponding to the reduction of Ru (IV) species to species with average oxidation states of 3.75 & 3.5 at the potentials of 0.35 and 0.15 V respectively.

In a study of Ru (IV) containing solutions, Wehner and Hindman (11) observed reactions at 0.96 and 1.16 V vs SCE on platinum, attributing the latter irreversible oxidation at 1.16 V to formation of RuO_4 from Ru (IV) and the process at 0.96 V to formation of a species with an average oxidation state of 4.38. Mousset (10) studied the electrovolatilisation from $\text{RuO}_2 \cdot x\text{H}_2\text{O}$ and commercial RuNO^{3+} solutions. $\text{RuO}_2 \cdot x\text{H}_2\text{O}$ showed no reduction processes at ~0.4 and 0.9 V vs. Ag/AgCl, in good agreement with Maya's (14) reported reduction potentials. Mousset's electrovolatilisation studies on RuNO^{3+} solutions indicated oxidation processes at 1.1V and 1.5 V vs. Ag/AgCl attributed to RuO_4 generation reactions.

However, the data summarised in Table 1 has several issues with regards to the oxidation behaviour of Ru (III). Notwithstanding the lack of consensus regarding peak assignment, especially those relating to higher oxidation state transitions, much of the data relates to the reduction of solution phase Ru (IV), with the oxidation behaviour of the generated reduction product being indirectly inferred; this is complicated by the product rarely being monomeric Ru (III) but rather Ru(III)-Ru(IV) oligomers (vide supra). Additionally, a number of the studies cited are conducted using Au or Pt electrodes, systems that have two limitations with respect to study of the Ru(III) system: (i) oxygen evolution as a result of water oxidation on Au or Pt occurring at ~0.99 V vs. SCE at pH 0, potentially masking higher potential oxidation reactions of Ru such as Ru (IV) to Ru (VIII) under conditions relevant to HAL chemistry, see figure 1 (16); and (ii) especially for gold, the assignment of peaks observed in the cyclic voltammetry of Ru(III)/Ru(IV) solutions at lower potentials than oxygen evolution being complicated by the intrinsic electrochemistry of the electrode itself. The latter includes gold oxide formation and stripping peaks which occur in the range +1.24 to +1.41 V and 0.55 to 0.75 V vs SCE respectively, and the oxidation and reduction of so-called Burke sites (a sub-monolayer of low coordination state Au atoms at the gold electrode surface (17-19) which occur in the range 0.4 to 0.6 V vs SCE at pH 0 (20) and so overlap, and may be confused with, many of the monomeric and oligomeric Ru(III)/Ru(IV) in this range (see Table 1).

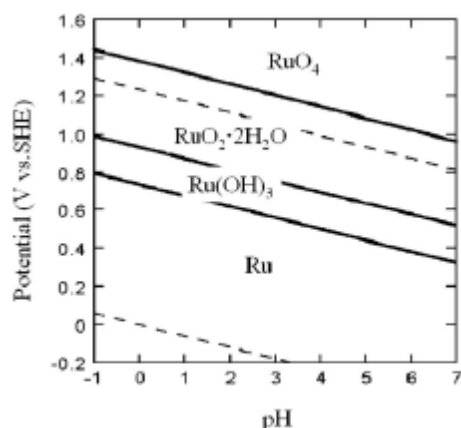


Figure 1: Eh-pH (Pourbaix) diagram for the Ru-H₂O system (taken from ref. 16)

Unfortunately, extant thermodynamic data related to Ru redox chemistry are not helpful here. Fig 1&2 show both the Ru-H₂O E_h-pH (Pourbaix) diagram (16) and Ru Latimer diagram (21), neither of which report on data related to Ru(III)/Ru(IV) redox couple where Ru(III) is present in the solution phase. Indeed, the Latimer diagram provides no data on the Ru(IV)/Ru(III) transition at all. Given these uncertainties, this paper presents a study of the behaviour of NO-free and NO complexed Ru (III) in order to understand the effect NO complexation has on the redox chemistry of Ru. Particularly, we study the oxidation reactions of RuCl₃ and RuNO³⁺ species at acidities relevant to HAL, seeking to characterise key redox transitions within both systems and also compare redox potentials observed at particular transitions. Coupled electrochemical / microgravimetric measurements are used to obtain a more robust view of what is occurring during the redox processes under study, especially in terms of solid phase formation and loss.

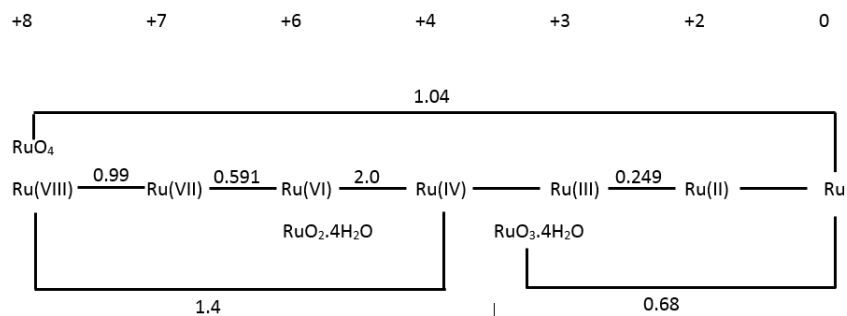


Figure 2: Ru Latimer diagram at pH 0

EXPERIMENTAL

Materials and reagents

All reagents were ACS reagent grade or higher and purchased from Fisher Scientific (Loughborough, UK) or Sigma Aldrich (Gillingham, Dorset, UK) and used without further purification. Doubly distilled water, further purified by a deionisation system (Epure model 04642, Barnstead/Thermodyne, Dubuque, IA, USA) to a resistivity of $1.8 \times 10^5 \Omega\text{m}$. Nitrogen (99.998% grade) was supplied by BOC Ltd. (Guilford, Surrey, UK).

RuCl₃.xH₂O solution preparation

Solutions of RuCl₃.xH₂O (10 mol dm⁻³) were made in HClO₄ (0.1 mol dm⁻³) made up with distilled water. Prior to electrochemical analysis, all solutions were purged with N₂ for 20 minutes to remove dissolved O₂.

RuNO(NO₃)₃ solution preparation

A commercially available RuNO(NO₃)₃ solution in HNO₃ was supplied by Johnson Matthey (Royston, Hertfordshire, UK) and was diluted by factor 3 and purged with N₂ for 20 minutes to remove dissolved O₂ prior to any electrochemical measurement being taken.

Exhaustive electrolysis

Electroreduction of as prepared RuCl₃ solutions, via exhaustive electrolysis, was carried out in a separated cell using an agar/ KClO₄ salt bridge, made with distilled water, under an inert N₂ atmosphere. The solution was left stirring for 12 hours at 0.2 V. Pt wire mesh was used as a working electrode (Goodfellow Cambridge Ltd., Huntingdon, UK.)

Electrochemical measurements

All electrochemical measurements, unless otherwise stated, were made using a freshly polished glassy carbon (2.9 mm diameter) working electrode in a 3 electrode cell with a Pt wire mesh (Goodfellow Cambridge Ltd., Huntingdon, UK) counter electrode and a Ag/AgCl (Alvatek Ltd. Tetbury, Gloucestershire, UK) reference electrode used in a double junction (Alvatek Ltd. Tetbury, Gloucestershire, UK) configuration with saturated K₂SO₄ solution. The working electrode was polished using decreasing grades of diamond slurries (6, 3, 1 μm) (Macron) with a final polish on a clean polishing pad soaked in distilled water. After polishing, the electrode was sonicated for 30s at 20W power in ethanol then distilled water to remove any debris remaining from polishing stages. All measurements were conducted at room temperature and under an inert N₂ atmosphere.

Electrochemical microgravimetric measurements

The electrochemical quartz crystal microbalance (EQCM) is a well-established method for the measurement of small changes in electrode mass due to reactions occurring at the electrode-solution interface. A detailed description of QCM theory may be found in various texts (21-24). Assuming mass is rigidly bound; the

measured shift in the resonant frequency is converted to a mass change via the Sauerbrey equation, Equation [1]

$$\Delta f = -Cf\Delta m \quad (\text{Eq.1})$$

Where Δf is the change in resonant frequency (Hz), Δm is the mass change (g) and Cf is the sensitivity constant. The value of Cf can be determined from electrochemical deposition and dissolution of copper via cyclic voltammetry (25, 26) we have found it to be 0.059 Hz (ng cm²), which is in excellent agreement with a theoretical value of 0.056 Hz (ng cm⁻²) quoted by the manufacturer (Q-sense, Biolin Scientific, Manchester, UK).

EQCM experiments used quartz crystals (SciMed Ltd., Stockport, Cheshire, UK) coated with amorphous carbon, 14 mm diameter, AT cut with a 10 MHz resonant frequency. Experiments were performed in a ground floor lab sited directly on building foundations and isolated from heavy machinery and vibration sources.

Analysis

All electrochemical measurements, unless otherwise stated, were made using an Autolab potentiostat PGSTAT128N equipped with a low current amplifier (Metrohm UK Ltd., Runcorn, Cheshire, UK). EQCM experiments were collected using a Gamry Potentiostat model 600, coupled with a Gamry EQCM model 10M (SciMed Ltd., Stockport, Cheshire, UK) allowing simultaneous QCM and potentiometric measurements to be taken. Ultraviolet visible (UV-vis) spectroscopy was carried out with a Gamry spectro-115 spectrometer (SciMed Ltd., Stockport, Cheshire, UK) with a 1 cm path length quartz cuvette. All measurements, unless otherwise stated, were conducted in 0.1 mol dm⁻³ HClO₄ and spectra were referenced to a 0.1 mol dm⁻³ HClO₄ solution.

RESULTS AND DISCUSSION

In order to provide a direct comparison between the work presented with that in the literature (see Table 1), Ru (III) electrochemistry was first studied by running a cyclic voltammogram (CV) of a solution of as-received RuCl₃ in HClO₄ using a 250 μm diameter gold micro disc as working electrode. Fig. 3 shows a full CV recorded over the range -1 to +2 V vs Ag/AgCl as well as an expanded scale inset showing the features in the range -0.15 to 0.8V. The oxidation peak at 1.1 V is co-incident with gold oxide formation at pH 1 (20), while the Ru-H₂O E_h-pH diagram and Latimer diagram of Fig. 1 & 2 indicate that it may have a significant component associated with Ru (VIII) evolution. The inset of Fig.3 shows a reduction peak at ~-0.7 V which we assign to interfering gold oxide stripping (20).

It also reveals the presence of apparently reversible processes at 0.25 and 0.4 V. These are in close accord, both in appearance and position, with voltammetric features reported by Maya (12) who reported reversible peaks at 0.15 and 0.35 V during a study of the reduction of Ru (IV) solutions using a platinum working electrode. Maya assigned these to reactions involving Ru oligomers in the following average oxidation states: Ru (3.5)/ Ru (3.75) at 0.15 V; and Ru (3.75)/ Ru (IV) at 0.35 V, an assignment we therefore adopt for our peaks at 0.25 and 0.4 V. This

leads to the curious conclusions that (i) solutions of as received RuCl_3 exhibit no oxidation features attributable to free /monomeric Ru (III); and (ii) the voltammetry is dominated by Ru(III)- Ru(IV) oligomer electrochemistry – despite, nominally, there being no Ru(IV) initially present in the RuCl_3 solution under study.

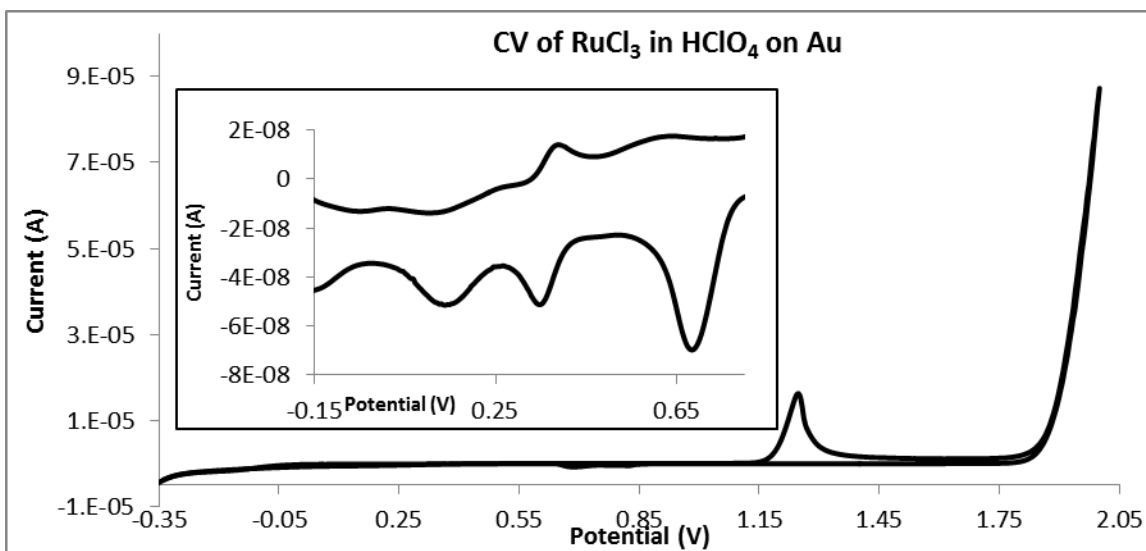


Figure 3: CV of 10 mol dm^{-3} RuCl_3 in 0.1 mol dm^{-3} HClO_4 using a Au working electrode ($250 \mu\text{m}$ diameter). Scan rate: 0.1 Vs^{-1} . Inset: expanded scale from -0.15 to 0.8 V.

In order to eliminate any potential interference from gold electrochemistry, the experiment of Fig.3 was repeated using a glassy carbon disc as working electrode, the resulting CV being shown in Fig. 4a. The observed voltammetric features are much more clearly resolved than in Fig. 3 with two peaks clearly visible at 0.55 and 0.9 V. Maya also reported a peak at 0.9 V which they attribute to tetramer oxidation, Ru (IV) to (4.38).

Given this result, and the apparent presence in the voltammetry of as-received RuCl_3 solutions of Ru(IV) species (Fig.3), the (nominally) RuCl_3 solutions used in Figs. 3 & 4 were analysed using UV-vis. spectroscopy, Fig. 4b, in order to identify Ru species initially present. Wehner & Hindman (9) and Yan *et al* (27) report that absorption bands for RuCl_3 appear at 400 and 525nm and for Ru (IV) at 475 and 310nm. All four bands are present in the UV-vis spectrum of Fig. 4b, confirming that a mixture of Ru in +3 and +4 oxidation states is present in solutions prepared from as-prepared RuCl_3 – indicating the Ru(III) species in this form has a high susceptibility towards aerial oxidation.

Thus, a 12 hour exhaustive electroreduction treatment at 0.2V (see experimental section above) was used to generate Ru (IV)-free RuCl_3 solutions. Fig. 4c shows a UV-vis. spectrum of a post-treatment RuCl_3 solution, confirming the loss of the Ru (IV) absorption bands at 475 nm and 310 nm. Fig. 4d shows the CV of the resultant solution from which it can be seen that the peak observed at 0.55 V in Fig. 4a has disappeared suggesting it was associated with the oxidation of Ru (IV) species or Ru (IV) containing oligomers. In contrast, the peak at 0.9 V in Fig. 4a is also observed in Fig. 4d, albeit slightly shifted to 0.85 V. Given the absence of Ru (IV)

species in the solution employed in the experiment of Fig. 4d, the peak at 0.85 V cannot be associated with tetramer oxidation as proposed by Maya. A further peak at ~1.2V is also seen in the CV of Fig. 4d.

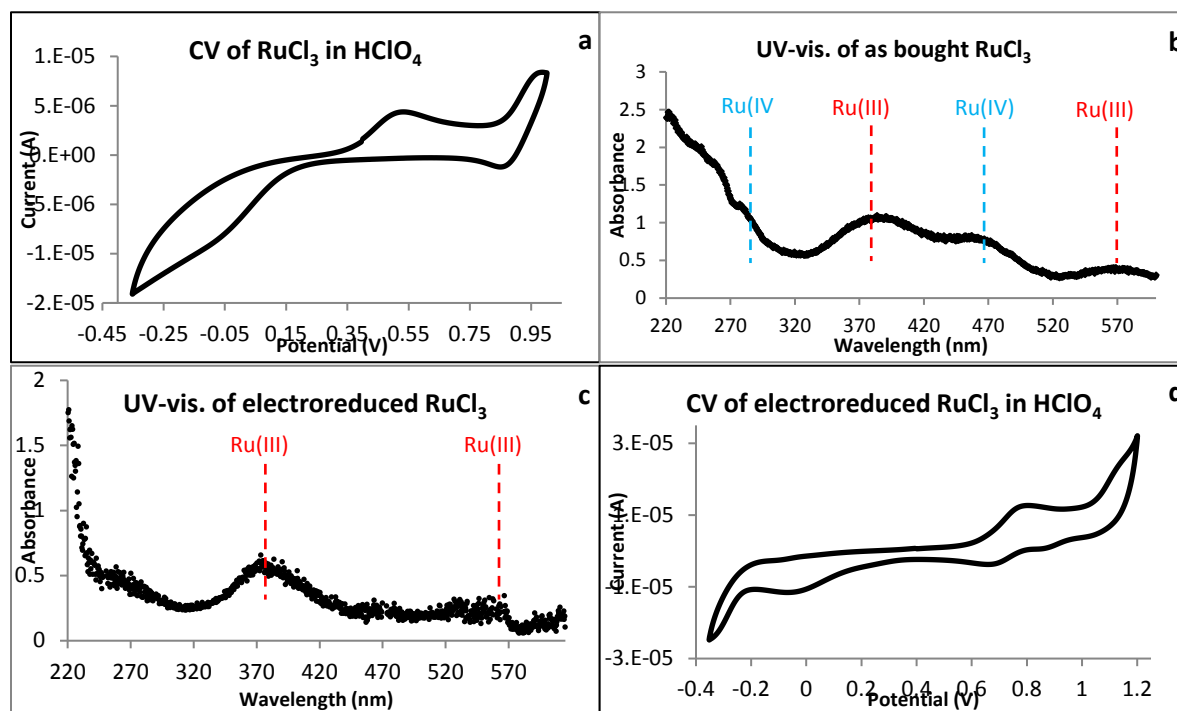


Figure 4: CV of RuCl_3 (10 mol dm^{-3}) in HClO_4 (0.1 mol dm^{-3}) Scan rate: 0.1 Vs^{-1} , b) UV-vis. spectrum of as bought RuCl_3 (100 mol dm^{-3}) in HClO_4 (0.1 mol dm^{-3}), c) UV-vis. spectrum of electroreduced RuCl_3 (100 mol dm^{-3}) in HClO_4 (0.1 mol dm^{-3}) d) CV of electroreduced RuCl_3 (10 mol dm^{-3}) in HClO_4 (0.1 mol dm^{-3}). Scan rate: 0.1 V s^{-1}

The peak at ~0.85 V was electrochemically interrogated using scan rate and Rotating Disc Electrode (RDE) studies. Analysis of the data using Randles-Sevcik and Koutecky-Levich equations, allowed for the calculation of the diffusion coefficient (D) and number of electrons (n) transferred in the transition. These calculations yielded values for n and D of 0.33 and $4 \times 10^{-10} \text{ m}^2 \text{ s}^{-1}$, respectively. An n number of 0.33 is strong evidence for the peak at ~0.85 V in Fig. 4d being associated with formation of a ruthenium trimer in the form; Ru (III) – Ru (IV) – Ru(III) from a solution of Ru (III).

To further study both peaks at ~0.85 V and ~1.2 V in Fig. 4d, a combined CV/voltamassogram was recorded from the same electroreductively pretreated solution of RuCl_3 over the slightly wider potential window of -0.4 to 2 V using carbon coated QCM crystals. Fig 5a shows the first scan recorded from such a crystal upon immersion in RuCl_3 solution, from which a number of observations may be made from the forward going scan.

The first is that, as well as the peaks observed at 0.85 V and 1.2 V in the CV of Fig.4d, a third peak with a substantially higher peak current than either of the other

two peaks is observed with an onset of ~ 1.3 V; this plateaus at ~ 1.7 V, just before the onset of a the displaced O_2 evolution wave on carbon. The second observation is that the peak at 0.85 V has no mass change associated with it in the voltamassogram trace, again suggesting that this peak is associated with a wholly solution phase process at the electrode surface, albeit one that results in the formation of an apparently soluble trimer species. The third observation is that the voltammetric peak at 1.2 V has a small mass increase associated with it whilst that at 1.3 V is associated with a similar, but opposite, mass loss. Inspection of the Ru-H₂O E_n-pH diagram of Fig. 1 leads us to conclude that the mass increase at 1.2 V is due to RuO₂ formation at the carbon piezoelectrode surface. This is further oxidised almost immediately at 1.3 V as the so formed RuO₂ is converted to RuO₄, presumably evolved as a volatile gas. This latter assignment is supported by the fact that the peak current at 1.3 V is much larger than that at 0.85 V and 1.2 V – as might be expected if the peak at 1.3 V were associated with a 4 electron transfer Ru (IV) to Ru (VIII) transition compared to a 1 electron transfer Ru (III) to Ru (IV) reaction at 1.2 V and trimer formation with an average n value of 0.33 at 0.85 V.

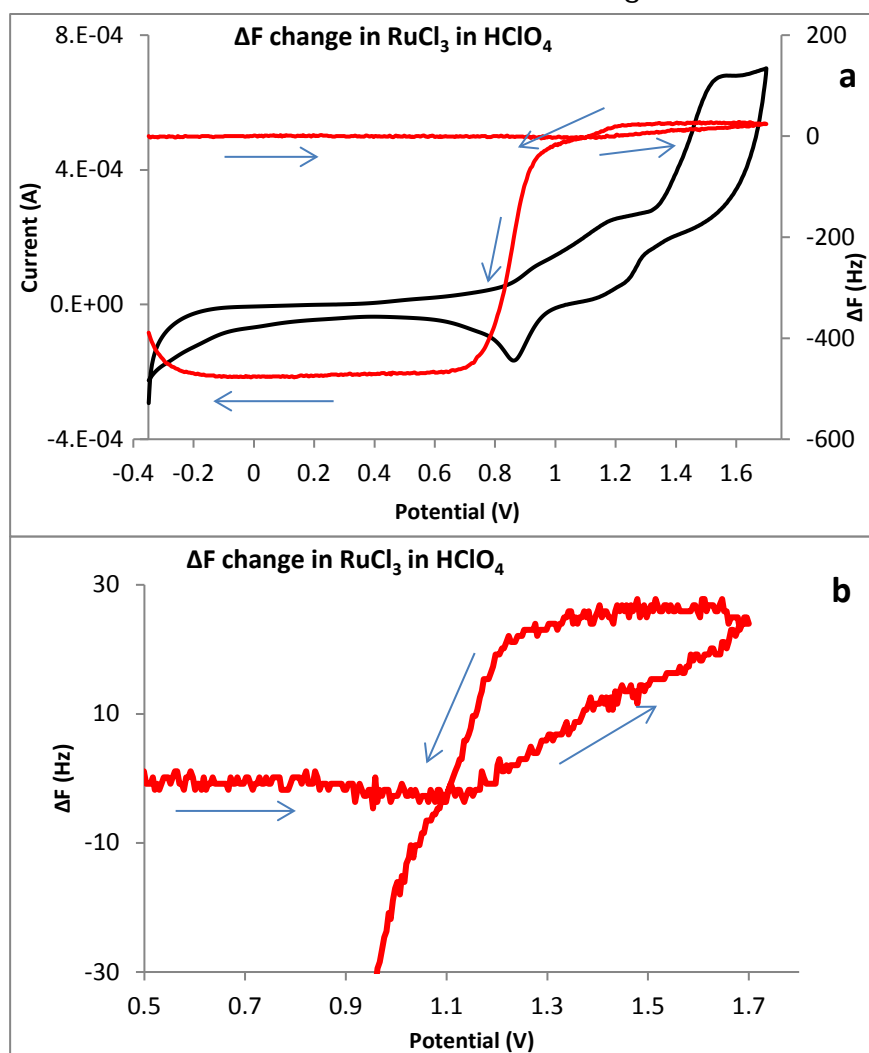


Figure 4: a) 1st scan cycle cyclic voltamassogram of same solution with the change in frequency of the crystal (red line), $v = 10 \text{ mV s}^{-1}$
 b) detail of frequency data from Figure 5a.

On the reverse scan, we see two mass gains at 1V and 0.8V. Upon consideration of the assignments in the forward going scan and the E_h -pH diagram of Fig. 1, the former feature may be associated with on oxidation of Ru (III) to RuO_2 , now giving rise to a mass increase due to the “switching off” of the following Ru(IV) to Ru(VIII) oxidation as the applied potential is decreased during the reverse scan); the latter feature is associated with a corresponding reduction in the voltammetric trace, it is thought this reduction could be the result of reduction of RuO_4^{2-} to RuO_2 at the piezoelectrode surface, giving rise to a resonant frequency decrease of the order of 500 Hz. It is stipulated that the origin of the RuO_4^{2-} is from the “switching off” of the Ru (IV) to Ru (VIII) transition; it is at this time that any remaining RuO_4 is then reduced to RuO_4^{2-} / RuO_2 .

These reverse scan assignments are further supported by the second consecutive CV scan cycle using the same carbon-coated piezoelectrode and RuCl_3 solution as used to gather the data of Figs. 5a and 5b. This second scan cycle is shown in Fig 6. Both of the mass increases / resonant frequency decreases seen in the reverse scan of Fig 5a are seen in Fig. 6 – first, a frequency decrease of ~ 100 Hz with a reverse scan onset of ~ 1.2 V and, second, a decrease of ~ 450 Hz with an onset of ~ 0.9 V. Both are associated with features in the corresponding reverse voltammetric trace – the decreases of 100 and 450 Hz with an oxidation peak at ~ 1.25 V and a reduction peak at ~ 0.9 V respectively. The features at 1.25 V are due to solution Ru (III) oxidation to solid RuO_2 , whilst those at 0.9 V are due to reduction of Ru (VI) to RuO_2 .

However, both the forward going microgravimetric and voltammetric traces of Fig. 6 exhibit differences to the corresponding traces of Figure 5a. The oxidation peaks at 1.2 V and $E > 1.3$ V are noticeably sharper in Fig. 6 than in Fig. 5a. The latter peak still has no mass change associated with it and so, based on its size relative to adjacent peaks and the assignment of Figure 5a, can again be attributed to the oxidation of RuO_2 to RuO_4 – this happening almost immediately after the RuO_2 has been formed from solution phase Ru (III). In contrast, in Fig. 6, the former peak at 1.2 V is concurrent with a frequency increase / mass decrease of ~ 300 Hz that is not seen in Fig. 5a. This can be explained by recalling that whilst the piezoelectrode presents a pristine carbon surface at the start of the first scan cycle, at the start of the second scan it is coated with a layer of RuO_2 during the first scan – suggesting that the frequency increase / mass decrease of ~ 300 Hz is due to the oxidation of RuO_2 to RuO_4 at 1.2 V. The Ru(III)/ RuO_2 oxidation may very well be occurring at ~ 1.2 V in Fig. 6; however, its associated current and mass change will be swamped by those associated with the RuO_2 stripping process.

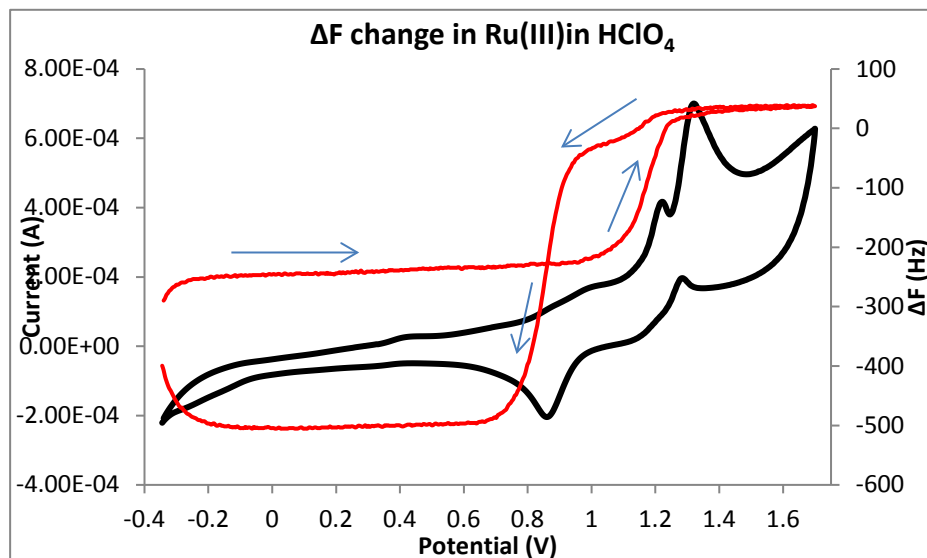


Figure 5: 2nd scan cycle cyclic voltammogram of same carbon coated piezoelectrode in the same 10 mol dm⁻³ RuCl₃ in 0.1 mol dm⁻³ HClO₄ solution used to record the data of Figs. 5a and 5b. Voltammetric data is shown in black, microgravimetry data (expressed as a change in the frequency of the crystal) shown in red, $\nu = 10 \text{ mV s}^{-1}$.

These assignments provide insights into the baseline behaviour of NO-free Ru redox chemistry. Having defined this, we then moved on to look at NO complexed Ru in the form of RuNO(NO₃)₃ to establish any differences in the redox behaviour due to NO complexation. For direct comparison, cyclic voltammograms were recorded over the same range, -0.4 to 2 V, as the RuCl₃ solution in fig. 5a and using the same carbon coated crystals. One such voltammogram is shown in fig. 7a and 7b; given the assignments made for the RuCl₃ system, these assignments were adopted in the RuNO³⁺ system as it is assumed the redox processes occurring in both systems will be similar. The peak at ~0.8 V in Fig. 7 has a corresponding frequency decrease suggesting this is formation of solid phase RuO₂, which is seen at 1.1 V in the RuCl₃ system, fig 5a. RuO₂ plated on the electrode surface is stripped off, assumed to be in the form gaseous RuO₄, at ~1.3 V. Once RuO₄ generation is "switched off," the frequency decrease between 1.7 and 1 V on the reverse trace is thought to be decomposition of RuO₄ to RuO₂. The frequency decrease/ mass increase at ~0.8 V on the reverse scan is associated with a reduction peak in the electrochemical trace in Fig. 7. This can be explained if when RuO₄ is "switched off" at 1.7 V it decomposes to a mixture of RuO₂ and RuO₄²⁻. At 0.8 V this RuO₄²⁻ then reduces to RuO₂, both explaining the reduction peak and mass increase at ~0.8 V in Fig 7.

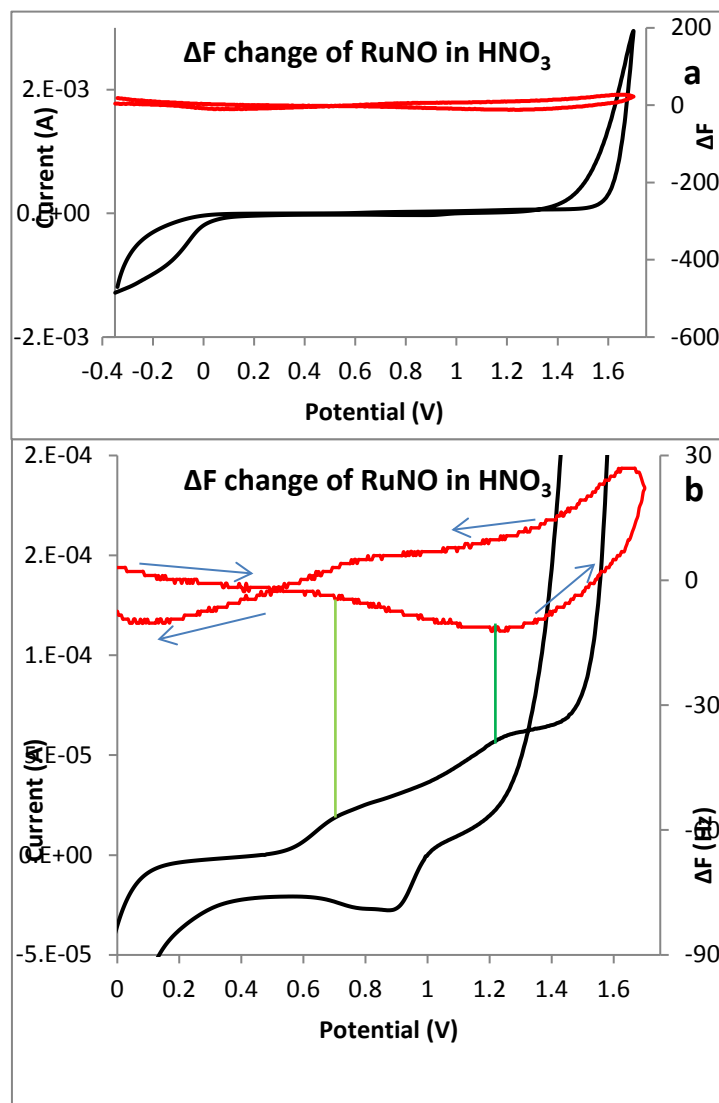


Figure 6: a) cyclic voltammogram of 125 mol dm⁻³ RuNO(NO₃)₃ in 2.5 mol dm⁻³ HNO₃. Electrochemical trace (black line) and the change in frequency of crystal (red line). $V = 10 \text{ mV s}^{-1}$ b) detail of cyclic voltammogram from fig. 7a

When comparing the RuNO³⁺ and RuCl₃ systems, two main observations can be made. The first is that the mass change associated with the redox processes occurring in the range 0.8 to 1.3 V are in the order of hundreds of Hz, in the RuCl₃ system, Fig. 5a. In the RuNO³⁺ system, Fig. 7, they fall to tens of Hz. The second concerns a change in the onset of volatile RuO₄ generation from Ru (III) in the RuNO³⁺ system, this occurs at ~1.3 V, Fig. 7, whilst in the RuCl₃ system it occurs at ~1.2 V, Fig.5a. Both of these observations suggest NO complexation does protect against Ru (III) oxidation and thus volatile RuO₄ generation. Our observed onset of volatilisation in the RuNO³⁺ system, ~1.3 V, is lower than that previously reported in literature. Mousset (10) reported RuO₄ generation reactions at 1.1 and 1.6 V from a solution of RuNO(NO₃)₃ however, our experiments seem to indicate that the peak at 1.1 V would be related to RuO₂ formation as we continue to see a

frequency decrease in our RuNO^{3+} system until ~ 1.3 V. Therefore, this would suggest the peak at 1.6 V in Mousset's work, is the peak related to RuO_4 generation and we see this in our system at ~ 1.3 V.

CONCLUSIONS

The electrochemistry of RuCl_3 in $0.1 \text{ mol dm}^{-3} \text{ HClO}_4$ has been investigated using combined CV and electrochemical microgravimetry experiments for the first time. As purchased RuCl_3 was found to contain Ru in the +3/+4 oxidation states and so required exhaustive electroreduction to the +3 state before use. Using carbon electrodes due to their wider aqueous solvent window and lower faradaic interferences, four features have been identified in the forward going scan of the CV of RuCl_3 and two in the reverse.

The forward going features are: at ~ 0.8 V, an oxidation with no accompanying electrode mass change and a mean electron number of 0.33 suggesting the formation from solution phase Ru(III) of a solution phase Ru(III)-Ru(IV)-Ru(III) trimer; at ~ 1.2 V during the first scan, an oxidation with an accompanying electrode mass increase, suggesting the deposition from Ru(III) solution phase species of solid RuO_2 ; also at ~ 1.2 V in the second scan, during which the carbon surface will be coated with a RuO_2 layer deposited during the first scan, an oxidation with an accompanying mass decrease due to the oxidation of RuO_2 to volatile RuO_4 ; and at $E > 1.3$ V, a large oxidation wave with little or no mass change associated with it which we assign to the almost immediate oxidation of the Ru (III) straight to volatile RuO_4 . The reverse going features are: at ~ 1.2 V, an oxidation with an accompanying electrode mass increase due to deposition of RuO_2 from Ru (III); and at ~ 0.9 V a reduction peak with an accompanying large electrode mass increase which we assign to the reduction of RuO_4^{2-} to RuO_2 .

Analogous studies of solutions of $\text{RuNO}(\text{NO}_3)_3$ show similar features with two key differences. The first is that the mass changes associated with the electrodeposition and stripping of RuO_2 in the potential range 0.8 to 1.3 V are significantly smaller for RuNO^{3+} solutions (i.e. Ru (III) complexed with NO) than those for solutions of RuCl_3 (i.e. Ru (III) that is not complexed with NO). The second difference is the potential for the onset of RuO_4 formation from RuNO^{3+} solutions is 100 mV positive of that for RuCl_3 solutions. Both observations suggest that NO complexation protects Ru (III) against oxidation and thus, to a certain extent, from ultimate volatilisation as RuO_4 .

ACKNOWLEDGEMENTS

All data created during this research are openly available from Lancaster University data archive at <http://dx.doi.org/10.17635/lancaster/researchdata/14>. We thank the UK Engineering & Physical Sciences Research Council (iCASE Award No 11440238) Sellafield Sites Ltd (NNL Agreement 10009355) and the Lloyd's Register Foundation for financial support. Lloyd's Register Foundation supports the advancement of engineering related education, and funds research and development that enhances safety of life at sea, on land and in the air.

REFERENCES

1. Z. Holgye, M. Krivanek, *J. Radioanal.Chem.*, 42, 133 – 141 (1978).
2. T. Sato, *J. Radioanal.Chem.*, 129, 77 - 84 (1989)
3. T. Sato, *J. Radioanal Chem.*, 139, 25 - 29 (1990)
4. P. W. Cains, K. C. Yewer, S. Waring, *Radiochim. Acta.*, 56, 99 – 104 (1992)
5. Y. Morris, A. Haig, *NNL Internal Communication*, 10, 10758, Issue 2 (2010)
6. Y. Morris, *NNL Internal Communication*, 10, 10750, Issue 2 (2010)
7. H. A. C. McKay, *BNFL Internal Report*, HAWGWP/P153 (1977)
8. P. W. Cains, AERE – R 9855 (1980)
9. D. Scargill, C.E. Lyon, N.R. Large, J.M. Fletcher, *J. Inorg. Nucl. Chem.*, 27, 161 - 171, (1965)
10. F. Mousset, F. Bedioui, C. Eysseric, *Electrochim. Comm.*, 6, 351 - 356 (2004)
11. P. Wehner, J. C. Hindman, *J. Amer. Chem. Soc.*, 72, 3911 - 3918 (1950)
12. L. W. Niedrach, A. D. Tevebaugh, *J. Amer. Chem. Soc.*, 73, 2835 - 2837 (1951)
13. D. K. Atwood, T. De Vries, *J. Amer. Chem. Soc.*, 84, 2659 - 2661 (1962)
14. L. Maya, *J. Inorg. Nucl. Chem.*, 41, 67 - 71 (1978)
15. R. M. Wallace, R. C. Propst, *J. Amer. Chem. Soc.*, 91, 3779 - 3785 (1969)
16. Y. Sugawara, A. P. Yadav, A. Nishikata, T. Tsuru, *J. Electrochem. Soc.*, 155, B897 – B902 (2008)
17. L.D. Burke, D.T. Buckley, J.A. Morrissey, *Analyst*, 119 841 - 845 (1994)
18. L.D. Burke, J.F. O'Sullivan, *Electrochim. Acta*, 37 585 – 594 (1992)
19. L.D. Burke, B.H. Lee, *J. Electroanal. Chem.*, 330 637 - 661 (1992)
20. S.G.D.Shackleford, C.Boxall, S.N.Port, R.J.Taylor, *J.Electroanal.Chem.*, 538-539, 109-119 (2002)
21. A. J. Bard, R. Parsons, J. Jordan, *Standard Potentials in Aqueous Solution*, CRC Press, 1985
22. D.A. Buttry, *Electroanal. Chem.*, 17, 1 - 85 (1991)
23. D.A. Buttry, *Electrochemical Interfaces: Modern Techniques for In-Situ Interface Characterisation*, H.D. Abruna, Editor, VHC Publishers Inc., 529-566, (1991)
24. M.R. Deakin, D.A. Buttry, *Anal. Chem.*, 61, 1147A-1154A, (2008)
25. C. Gabrielli, M. Keddam, R. Torresi, *J. Electrochem. Soc.* 138(9), 2657-2660 (1991)
26. G. L. Borges, K. K. Kanazawa, J. G. Gordan II, *J. Electroanal. Chem.* 364(1-2), 281-284 (1994)
27. X. Yan, H. Liu, K. W. Liew, *J. Mat. Chem.*, 11, 3387 - 3391 (2001)